# *Selecting the Optimal Fractional Frequency Reuse Scheme in Long Term Evolution Networks*

**Dimitrios Bilios, Christos Bouras, Vasileios Kokkinos, Andreas Papazois & Georgia Tseliou**

**Wireless Personal Communications**
An International Journal

ISSN 0929-6212
Volume 71
Number 4

Wireless Pers Commun (2013)
71:2693-2712
DOI 10.1007/s11277-012-0965-z

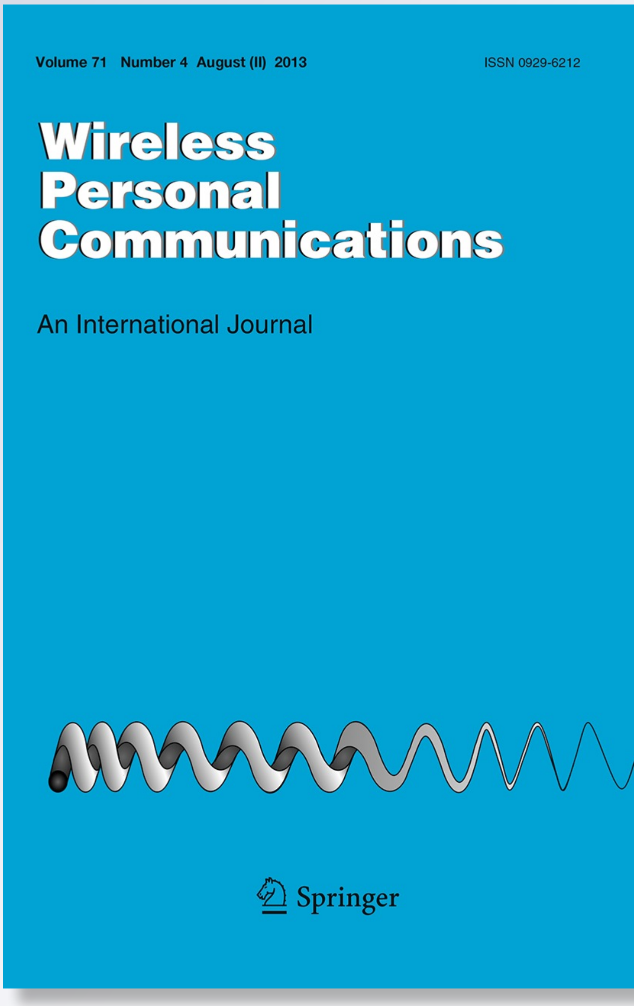


Springer

Wireless Pers Commun (2013) 71:2693–2712
DOI 10.1007/s11277-012-0965-z

# Selecting the Optimal Fractional Frequency Reuse Scheme in Long Term Evolution Networks

**Dimitrios Bilios · Christos Bouras · Vasileios Kokkinos · Andreas Papazois · Georgia Tseliou**

Published online: 5 February 2013


**Abstract** Long Term Evolution (LTE) networks offer high capacity and are specified and designed to accommodate small, high performance, power-efficient end-user devices. One limiting factor that influences LTE performance is the interference from neighbouring cells, the so called Inter-Cell Interference (ICI). The investigation of ICI mitigation techniques has become a key focus area in achieving dense spectrum reuse in next generation cellular systems. Fractional Frequency Reuse (FFR) has been proposed as a technique to overcome this problem, since it can efficiently utilize the available frequency spectrum. This manuscript proposes a dynamic mechanism that selects the optimal FFR scheme based on a custom metric, which is called user satisfaction. In detail, the proposed mechanism divides the cell into two regions, the inner and outer region, and selects the optimal size as well as the optimal frequency allocation between these regions with main target to maximize the user satisfaction metric. The proposed mechanism is evaluated through several simulation scenarios that incorporate users' mobility and its selected FFR scheme is compared with other frequency reuse schemes in order to highlight its performance.

**Keywords** Cellular networks · Long term evolution · Fractional frequency reuse · Orthogonal frequency division multiple access

D. Bilios · C. Bouras (✉)· V. Kokkinos · A. Papazois · G. Tseliou
Computer Technology Institute & Press "Diophantus", N. Kazantzaki, 26504 Patras, Greece
e-mail: bouras@cti.gr

D. Bilios
e-mail: bilios@cti.gr

V. Kokkinos
e-mail: kokkinos@cti.gr

A. Papazois
e-mail: papazois@ceid.upatras.gr

G. Tseliou
e-mail: tseliou@cti.gr

D. Bilios · C. Bouras · V. Kokkinos · A. Papazois · G. Tseliou
Computer Engineering and Informatics Department, University of Patras, 26504 Patras, Greece

## 1 Introduction

Orthogonal Frequency Division Multiple Access (OFDMA) has become an attractive technology for achieving high data transmission rate in wireless communication systems and it is part of various system standards for mobile communications. This happens because each terminal occupies a subset of subcarriers (called OFDMA traffic channel) and each traffic channel is assigned exclusively to one user at any time [1]. Therefore, OFDMA offers great spectrum efficiency and flexible frequency allocation to users. However, in Long Term Evolution (LTE) networks the system performance is severely hampered by the Inter-Cell Interference (ICI) due to the frequency reuse. For example, the cell edge users will experience high interferences from neighbouring cells. For this reason, Third Generation Partnership (3GPP) LTE is currently studying some policies to mitigate the ICI.

Fractional Frequency Reuse (FFR) is discussed in OFDMA-based networks to overcome the Co-Channel Interference (CCI) problems (where different radio transmitters use the same frequency) and ICI problems [1]. In FFR the cell space is divided into two regions: inner, which is close to the Base Station (BS) and outer, which is situated to the borders of the cell. The whole frequency band is divided into several sub-bands, and each sub-band is assigned either to the inner or the outer region of the cell. As a result of FFR, CCI is eliminated, and ICI is substantially reduced [2]. At the same time the system throughput is enhanced. Various reuse factors and interference mitigation levels can be achieved by adjusting either the bandwidth proportion assigned to each region or the transmission power of each band.

In LTE, OFDMA utilizes 15 KHz subcarriers, which are grouped in physical Resource Blocks (RB). Each RB contains 12 subcarriers equating to 180 KHz of spectrum. There are various options how these RBs can be allocated, as well as implemented for FFR schemes. These schemes are fundamentally based on allocating a number of these RBs in a sector. The main issue that occurs is that they limit the maximum throughput available to user—since they are not able to allocate the full bandwidth. In detail, OFDMA FFR, for interference mitigation, divides frequency and time resources into several resource sets (sub-bands). Typically, each resource set is reserved for a certain frequency allocation and is associated with a particular transmission power profile. FFR schemes can be considered both in uplink and downlink channels, but typically they are considered in the downlink. This can be explained due to the reduction of the complexity and the less required information. The use of FFR in cellular networks leads to natural trade-offs between enhancement in coverage and rate for the users found in outer region and overall throughput and spectral efficiency.

By utilizing interference avoidance schemes, the system tries to avoid collisions between the same frequencies used in neighbour cells. This can be done either in a static way by allocating different frequencies to neighbour cells (also called Frequency Reuse Factor (FRF) greater than one), or with an intelligent scheduler taking care of the collisions. Considering the signalling overhead and the complexity to implement the intelligent scheduler, only the static method is widely adopted in practical network deployments.

This manuscript proposes a dynamic mechanism that selects the optimal FFR scheme based on the relative throughput of a user compared to the throughput of the users in the same cell. The software implementing the proposed mechanism is available at [3]. This custom metric is called User Satisfaction (US) throughout this work. The proposed mechanism uses an algorithm that divides the cell into two regions (inner and outer) and calculates the US metric for successive combinations of the inner region radius and inner region frequency allocation. For each combination, besides the US metric, the algorithm calculates the per-user throughput and the cell total throughput. After these calculations, the mechanism selects the FFR deployment that maximizes the US metric.

The rest of this manuscript is structured as follows: Sect. 2 describes in detail the work related to our study. The basic theoretical background regarding FFR is explained in Sect. 3. Section 4 describes the procedure used for the calculation of throughput and US; while Sect. 5 describes the system model and provides an overview of the proposed mechanism. The evaluation of the mechanism and the simulation results are presented in Sect. 6. Finally, the conclusions and some ideas for future work are described in Sects. 7 and 8 respectively.

## 2 Related Work

FFR is based on the idea of applying a frequency reuse of one in areas close to the BS, and a higher reuse in areas closer to the cell border. It should be noted that the majority of the related work regarding FFR in the context of OFDMA systems, has mainly been discussed in cellular network standardization for 3GPP and Third Generation Partnership Project 2 (3GPP2) [4].

This idea was first proposed for Global System for Mobile Communications (GSM) networks (see work [5]) and has been adopted in the WiMAX forum (work [6]), but also in the course of the 3GPP LTE standardization where the focus lies on practically implementable algorithms [7,8]. Several variations of such schemes are possible.

Recent research on FFR has focused on the optimal design of FFR systems by utilizing advanced techniques such as graph theory and convex optimization to maximize network throughput [9–11]. Additionally, the work presented in [12] considers spectral efficiency and the authors find the optimal frequency partitions in a two-stage heuristic approach. The novel aspect of this paper is the consideration of several metrics including network throughput, spectral efficiency and average cell-edge user Signal to Interference plus Noise Ratio (SINR), instead of optimizing the design for only one metric. Additionally, this paper presents an analytical framework used to evaluate outage probability for cell-edge users in Strict FFR and Soft Frequency Reuse (SFR) systems which is an important metric to consider since it can have a large impact on cell-edge user Quality of Service (QoS) and when combined with resource efficiency, can give an overall picture of cell/network capacity.

Recently, some promising flexible spectrum reuse schemes have been proposed such as the SFR scheme adopted in the 3GPP-LTE system (works [13,14]) and the FFR scheme presented in [15]. Among them, the SFR scheme can overcome severe ICI problems from adjoining cells at a cell-edge region, by emphasizing a part (called as the primary band) of the available radio spectrum and allocating it preferentially for cell-edge users. However, it still may incur even severer ICI to some of cell-edge users, because the high-powered primary band can accommodate only a pre-defined number of cell-edge users, while the remaining cell-edge users may be allocated to limitedly -powered secondary bands.

The conventional SFR scheme is based on hard reservation, which partitions the resource region into two orthogonal portions, one solely dedicated to users in the cell center and the other solely dedicated to those in the cell edge. This kind of resource allocation which restricts resource region to each user can ensure an SINR gain in average manner. As described in [16,17], however, it hurts a multi-user diversity gain and fairness of resource allocation, especially when the users are not uniformly distributed throughout the coverage. These problems can be handled by a soft reservation mechanism, which allows for sharing a whole resource region among all or some users. By employing soft reservation, the wider resource region leads to a more multi-user diversity gain and fairer resource allocation [16,17]. However, it is not straightforward to guarantee the average SINR gain.

This manuscript presents an extended analysis of the above studies, which is differentiated at several levels. More specifically, the contribution of this work includes an improved, dynamic mechanism that selects the optimal FFR scheme based on the US metric. The comparison of the selected FFR scheme with other already standardized frequency reuse schemes includes experiments with static and mobile users and highlights the improved performance of the mechanism.

## 3 Fractional Frequency Reuse

In FFR, in order to ensure that the mutual interference between users and BSs remains below a harmful level, adjacent cells use different frequencies. In fact, a set of different frequencies is used for each cluster of adjacent cells. Cluster patterns and the corresponding frequencies are reused in a regular pattern over the entire service area. The closest distance between the centres of two cells using the same frequency (in different clusters) is determined by the choice of the cluster size and the layout of the cell cluster. This distance is called the frequency reuse distance.

One of the main objectives of LTE is to achieve high spectral efficiency, meaning the use of the whole of the system's bandwidth in all cells. This approach is called Frequency Reuse 1 and is considered as the simplest frequency reuse scheme: all sub-bands of the available bandwidth are allocated to each cell. In Frequency Reuse 3, the system bandwidth is divided into 3 equal sub-bands; each one of these is allocated to cells in a manner that no other surrounding cell is using the same sub-band. Full frequency reuse in each cell can exempt the necessity of advance frequency planning among different cells, and the frequency reuse patterns can be dynamically adapted on a frame-by-frame basis in each cell. In this work a sub-case of these approaches is studied and analysed below.

At a first stage, an LTE multi-cellular network is defined. Our main objective is to apply FFR in order to improve the SINR and throughput and simultaneously reduce CCI and ICI. An indicative topology and frequency band allocation are depicted in Fig. 1. If the central BS is considered (blue colour), it can be assumed that most of the interference is caused by the six direct neighbours.

The topology of Fig. 1 consists of 7 cells and there are four resource sets. Each cell of the topology is divided into two regions; inner and outer region. The total available bandwidth of the system is split into four uneven spectrums (or resource sets), denoted by A (blue), B (green) C (red) and D (yellow). Spectrums A, B, and C have equal bandwidth and are allocated in outer regions with Frequency Reuse 3. On the other hand, spectrum D is allocated in all inner regions with Frequency Reuse 1. The frequency resources in all inner regions are universally used, since the inner region users are less exposed to ICI.

From user perspective Integer Frequency Reuse (IFR) can be regarded as a special case of FFR. In, IFR all RBs allocated to a cell can be used anywhere in the cell without any specification of user's location. However, reutilization of RBs in network cells may be one or greater.

For comparison reasons, the FFR scheme that is selected by our mechanism is compared with two different cases. The first case, where the cell bandwidth equals the whole network bandwidth, is called IFR with frequency reuse 1 (IFR1). In the second case, the inner region radius is zero and each cell uses one third of the network's bandwidth. This case is called IFR with frequency reuse 3 (IFR3). The difference with the IFR1 case, lies in the fact that only co-channel BS are considered in interference calculation and as a consequence, the interference BS density is divided by 3. The notation of IFR schemes is defined according to the work presented in [18].

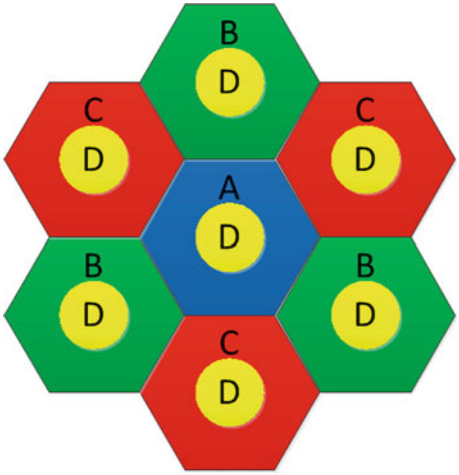


**Fig. 1** Proposed frequency band allocation

## 4 Calculation of Throughput and User Satisfaction

In this section we describe the theoretical approach to calculate the SINR, throughput and US metric. We assume that the overall network is composed of $N$ adjacent cells. Each cell contains a number of users seeking to share a group of subcarriers. We distinguish the case where a user is found in the inner or in the outer region of the cell. In a typical OFDMA cellular network, for a user $x$ who is served by a base station $b$ on subcarrier $n$, the related SINR is given by the following equation [19]:

$$SINR_{x,n} = \frac{G_{b,x} \cdot P_{b,n} \cdot h_{b,x,n}}{\sigma_n^2 + \sum_{j=1}^{k} G_{j,x} \cdot P_{j,n} \cdot h_{j,x,n}} \tag{1}$$

In (1), $G_{b,x}$ refers to the path loss associated with the channel between user $x$ and base station $b$, $P_{b,n}$ is the transmit power of the base station on subcarrier $n$, $h_{b,x,n}$ is the exponentially distributed channel fast fading power and $\sigma_n^2$ is the noise power of the Additive White Gaussian Noise (AWGN) channel. Symbols $k$ and $j$ refer to the set of all the interfering BSs (i.e. BSs that are using the same sub-band as user $x$). In detail, $j$ is the cell index and $k$ the number of co-channel cells. In our analysis, we assume that equal transmit power is applied, $P_{b,n} = P$ for all BSs. The coefficient $h_{b,x,n}$ is replaced by its mean value ($h_{b,x,n} = 1$) in Eq. (1).

The interference that occurs comes from disjoint sets of downlinks in the inner and outer region. A transmission in an inner region that is assigned specific frequency band causes interference only to inner users of other cells that are assigned the same band. Furthermore, it is necessary to distinguish two categories of BSs. The first consists of all interfering BSs transmitting to inner region users on the same sub-band as user $x$ and the second consists of all interfering BSs transmitting to cell-edge users on the same sub-band as user $x$.

After the SINR estimation, we proceed with the throughput calculation. The capacity of user $x$ on subcarrier $n$ can be calculated by the following equation [20]:

$$C_{x,n} = \Delta f \cdot \log_2(1 + SINR_{x,n}) \tag{2}$$

where, $\Delta_f$ refers to the available bandwidth for each subcarrier divided by the number of users that share the specific subcarrier. Moreover, the throughput of the user $x$ can be expressed as follows:

$$T_x = \sum_n \beta_{x,n} \cdot C_{x,n} \tag{3}$$

where, $\beta_{x,n}$ represents the subcarrier assigned to user $x$. When $\beta_{x,n} = 1$, the subcarrier $n$ is assigned to user $x$. Otherwise, $\beta_{x,n} = 0$.

Moreover, in order to evaluate the simulation experiments we define the metric User Satisfaction (US) as the sum of the users' throughput divided by the product of the maximum user's throughput and the total number of users ($X$) in the cell. This metric expresses the relative throughput of a user compared to the throughput of the users in the same cell and it physically presents how close the user's throughput is to the maximum throughput in the area. Specifically:

$$US = \frac{\sum_{x=1}^{X} T_x}{\max\_user\_throughput \cdot X} \tag{4}$$

US ranges between 0 and 1. When US approaches 1, all users in the corresponding cell experience similar throughput, while when US approaches 0, there are big variations in the throughput achieved by the users in the cell. US has been selected as performance metric since it leads to a fairer overall network behaviour. Indeed, as presented in [21], US results in similar values of users' throughput, irrespectively of their location in the cell.

## 5 System Model and Mechanism Overview

The proposed mechanism assumes a topology that consists of a grid of cells and a number of multicast users that are randomly distributed throughout the topology. The frequency allocation is examined in terms of RBs, the minimum allocation unit in LTE both for protocol side and system resource allocation [22]. In order to find the optimal FFR deployment (inner region radius and inner region frequency), the mechanism uses an algorithm which divides each cell into two regions and calculates the total throughput and US for the following 26 Frequency Allocations (FAs), assuming 25 RBs and that Frequency Reuse 1 and 3 are applied in the inner and the outer region respectively:

- $FA_1$: All (25) RBs are allocated in inner region.
  No RBs are allocated in outer region.
- $FA_2$: 24 RBs are allocated in inner region.
  1/3 RBs allocated in outer region.
- …
- $FA_{25}$: 1 RB allocated in inner region.
  24/3 RBs allocated in outer region.
- $FA_{26}$: No RBs allocated in inner region.
  25/3 RBs allocated in outer region.

The general case of the frequency allocation for the proposed mechanism is graphically presented in Fig. 2. The cell is divided in two regions: inner and outer. In Fig. 2b, $N$ refers to the total number of RBs. This means that for the case of $N = 25$ RBs, there are 26 FAs in total.

In the first place the proposed mechanism takes as input the network configuration, i.e. the amount of cells that will be generated per row and per column, the number of total network users, the network's bandwidth and the transmitting signal power of macrocells. Then the mechanism generates the network's deployment according to these parameters.

For each frequency allocation, the proposed mechanism calculates the per-user throughput, the cell total throughput and US. This procedure is repeated for successive inner region radius

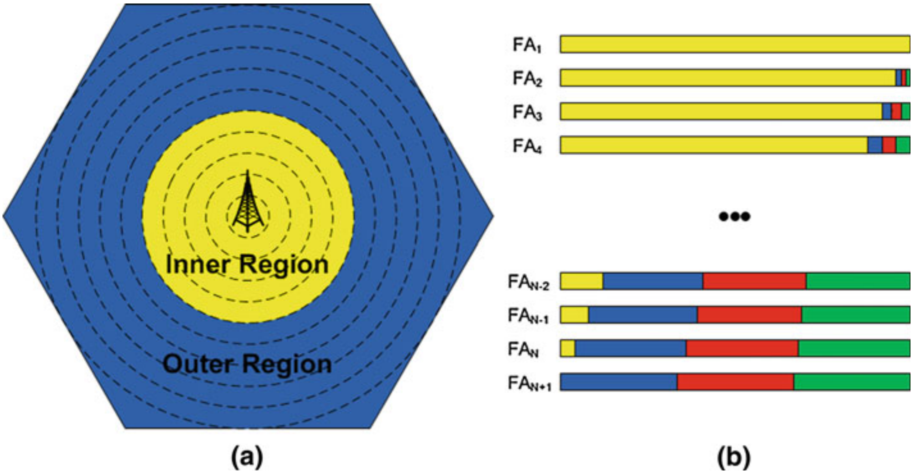


**Fig. 2** **a** Cell division and **b** frequency allocations of the mechanism

(0 to $R$, where $R$ is the cell radius). After the above calculations, the mechanism selects the FFR scheme that maximizes the US.

This procedure is repeated periodically in order to take into account user's mobility. Therefore, the per-user throughput, the cell total throughput and US are calculated in periodic time intervals (the exact time is beyond the scope of this manuscript) and at each time interval, the FFR scheme that maximizes the above parameters is selected. This periodic process is called adaptation.

```
% Algorithm
get_network_cells_&_users_parameters()  % get parameters about
                                        % cells and users
generate_network_cells_&_users()    % define topology and user
                                    % distribution
for  r = 0:stepR:R        % scan inner region radius
  for  n = 0:N            % scan inner region RBs
    for  x = 1:X          % users
      update_network()    % update network according to new
                          % RB allocation and inner
                          % region radius
      calculate_sinr(x)             % based on equation (1)
      calculate_capacity(x)         % based on equation (2)
      calculate_throughput(x)       % based on equation (3)
    end
    calculate_total_throughput(r,n)
    calculate_user_satisfaction(r,n)  % based on equation (4)
  end
end
calculate_ffr_for_max_user_satisfaction() % select r,n values
                                          % that maximize the
                                          % US metric
perform_adaptation_process()   % periodically repeat the above
                               % procedure in order to take
                               % into account users' mobility
output_plots()                 % export the proper figures
```

The pseudo-code of the algorithm is illustrated above and the software implementing the proposed mechanism is available at [3]. The tool is implemented in Matlab computing language and interactive environment for numerical computation and simulations. The complexity and the running time of the algorithm are proportional to the number of users, the number of cells in the topology, the number of RBs and the number of the inner region radius that are examined, i.e. $O(\#users \cdot \#cells \cdot N \cdot \#steps)$.

## 6 Performance Evaluation

This section evaluates the performance of the proposed mechanism. The main simulation parameters that were considered for the experiments are presented in Sect. 6.1. Section 6.2 investigates the values of throughput and US after the application of the proposed mechanism and Sect. 6.3 assesses the performance of the proposed mechanism for a scenario with moving users by comparing the performance of the selected FFR scheme with other frequency reuse schemes.

### 6.1 Simulation Parameters

The simulation parameters that are necessary for the conduction of the experiment are presented in Table 1. Since we examine an LTE-based cellular environment all the performance requirements, link and system simulation parameters (BS transmit power, Power Noise Density, Cell radius) are in accordance with the 3GPP specifications [22]. In detail, we consider a system with 5 MHz of bandwidth (i.e. LTE) divided into 25 RBs. Each RB has 12 subcarriers of 15 KHz each [23]. The scenario assumed is urban macro, which exists in dense urban areas, served by macrocells BS of 2,000 MHz frequency. In addition, we calculate the path loss according to Cost 231 Hata Model, which illustrates the highest path loss in urban areas [24,25]. Since the correlation in shadowing can significantly affect the mobility behaviour and the received power, and has impact on the overall system performance, we also consider the correlation distance of shadowing, which for our modelling is set to 40 m [20].

### 6.2 Scenario 1: Static Users

The scenario assumes that 360 static users are distributed uniformly in the topology, which consists of 16 cells (Fig. 3). We will focus on one cell of the topology that is highlighted in Fig. 3. The specific cell contains 24 users.

As depicted in Fig. 3, the selected FFR scheme that maximizes the US for the examined cell consists of two regions. The inner region (yellow) has 131 m radius and contains 6 users

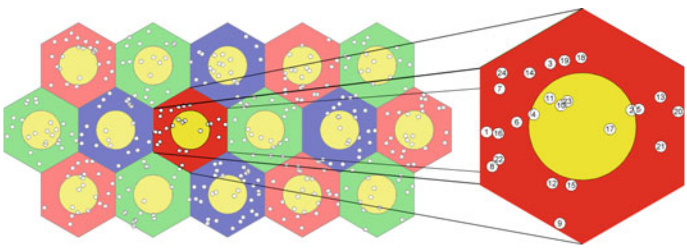

**Fig. 3** Optimal FFR scheme selected by the mechanism (inner region radius = 131 m)

**Table 1** Simulation parameters

| Parameter | Units | Value |
|---|---|---|
| System bandwidth | MHz | 5 |
| Resource blocks # | | 25 |
| Subcarriers # | | 300 |
| Subcarriers' bandwidth | Hz | 15 |
| Carrier frequency | MHz | 2,000 |
| Cell radius | m | 250 |
| Correlation distance | m | 40 |
| Channel model | | 3GPP Typical urban |
| Users' speed | km/h | 3, Pedestrian A |
| Path loss | dB | Cost 231 Hata Model |
| BS transmit power | dBm | 46 |
| Power noise density | dbm/Hz | −174 |

while the remaining cell area (red) constitutes the outer region and contains 18 users. In addition, the optimal bandwidth allocation for the inner region is 2 RBs. For the facilitation of the description of the experiments that follow, in Fig. 3 we number the users that are located in the examined cell.

### *6.2.1 Scenario 1: Selection of Optimal FFR Scheme*

This paragraph presents the operation of the mechanism during the selection of the FFR scheme that maximizes the US. More specifically, Figs. 4 and 5 present the US and the cell total throughput as a function of the inner region bandwidth and the inner region radius respectively. As mentioned, the proposed mechanism examines successive combinations of the inner region bandwidth and radius and selects the combination that maximizes the US metric. We have to remind that as US metric approaches 1 there are small differences between the values of users' throughput in the examined cell.

More precisely, Fig. 4 shows the way that the cell total throughput and US change as the number of the inner region RBs increases. These values correspond to the optimal inner region radius, which equals to 131 m. According to the figure, as the RBs allocated to the inner region increase from 0 to 25, the US increases and reaches its maximum value (0.7116) for 2 RBs. Higher values of inner region RBs lead to US decrement, while the allocation of all the available bandwidth to the inner region leads to the minimum value of US.

In Fig. 4, the curve that depicts the cell total throughput has also been included. Our goal is to observe how it changes when the number of RBs allocated in the inner region increases. However, the scope of this work is to maximize the US and not the cell total throughput. Consequently, as far as the cell total throughput is concerned, Fig. 4 shows that it decreases linearly as the inner region bandwidth increases.

Figure 5 depicts how the cell total throughput and US change as the inner region radius increases. In this case, the mechanism has already selected the optimal inner region RB allocation, which equals to 2 RBs. Therefore, Fig. 5 confirms the fact that the optimal FFR scheme corresponds to the deployment with 131 m radius and 2 RBs allocated to the inner region. This combination results in the maximum US value that equals to 0.7116.

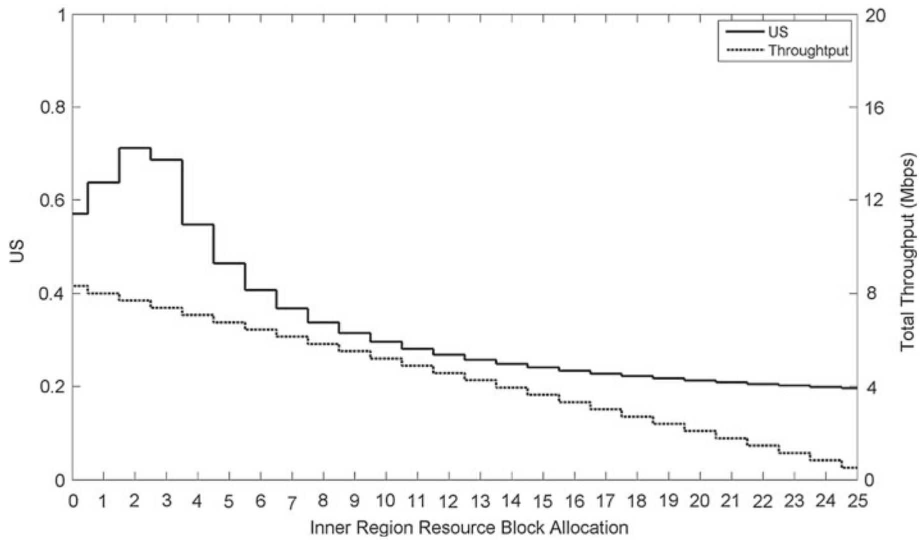


**Fig. 4** US and cell total throughput versus inner region RB allocation (inner region radius = 131 m)

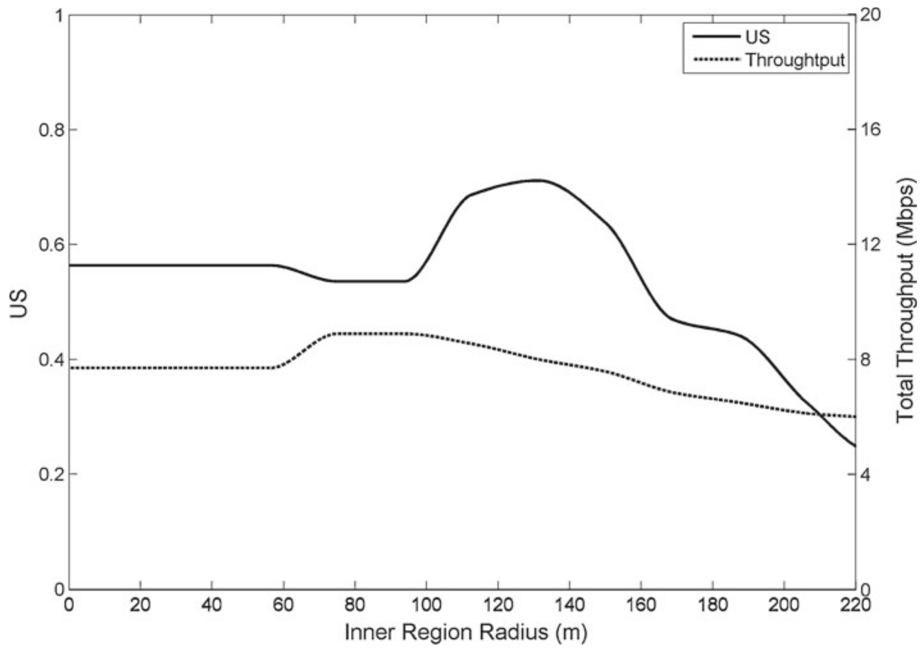


**Fig. 5** US and cell total throughput versus inner region radius (inner region RBs = 2)

In order to understand the behaviour of the cell total throughput in this case, the corresponding curve has also been included in Fig. 5. As Fig. 5 depicts, the highest value of cell total throughput (that is achieved for 2 RBs in the inner region) is 9.69 Mbps and appears when the inner region radius equals to 72 m. On the other hand, for 131 m inner region radius

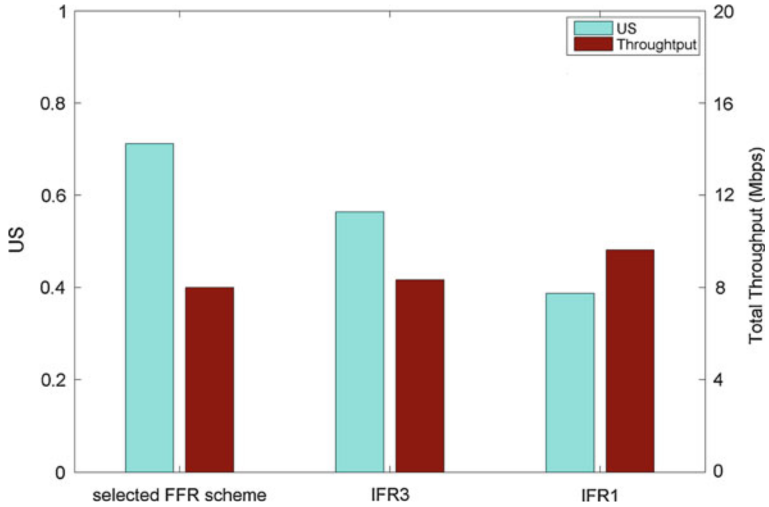


**Fig. 6** Comparison of IFR1, IFR3 and selected FFR scheme for the static users' scenario

(where US is maximized) the achieved cell total throughput is 8 Mbps. Although, this value is not the maximum achieved, it is very close to the maximum.

### *6.2.2 Scenario 1: Comparison of Selected FFR Scheme with IFR1 and IFR3*

This section makes a direct comparison between the frequency reuse schemes that were presented in Sect. 3 (IFR1, IFR3 and the FFR scheme selected by the proposed mechanism) in terms of US and cell total throughput.

Figure 6 presents the US for the three distinct scenarios. Many interesting observations arise from this figure. As far as the US metric is concerned, the selected FFR scheme results in higher values compared to the other two schemes. Indeed, IFR1 achieves a maximum US value equal to 0.3867 while IFR3 results in 0.5639 US. On the other hand, the selected FFR scheme achieves a maximum US value equal to 0.7116, i.e. 84.02 % increment compared to IFR1 and 26.19 % increment compared to IFR3. These percentages indicate the improved performance of the selected FFR scheme, and consequently of the proposed mechanism, in terms of US.

In order to further compare the three schemes, Fig. 6 also depicts the cell total throughput that each scheme achieves. IFR1 achieves the highest cell total throughput value (9.69 Mbps), IFR3 results in 8.3 Mbps cell total throughput while the selected FFR scheme achieves 8 Mbps for the selected inner region radius and frequency allocation. However, the fact that it achieves the highest US indicates that all users experience close throughput values and therefore avoids to distinct between "high-throughput" and "low-throughput" users.

## 6.3 Scenario 2: Moving Users

In this section we investigate the mechanism's behaviour, while selecting the FFR scheme that maximizes the US in a scenario with moving users. The topology and the initial user distribution are the same with the previous experiment. Similarly to the previous scenario, we focus on the highlighted cell of the topology presented in Fig. 3. During the experiment

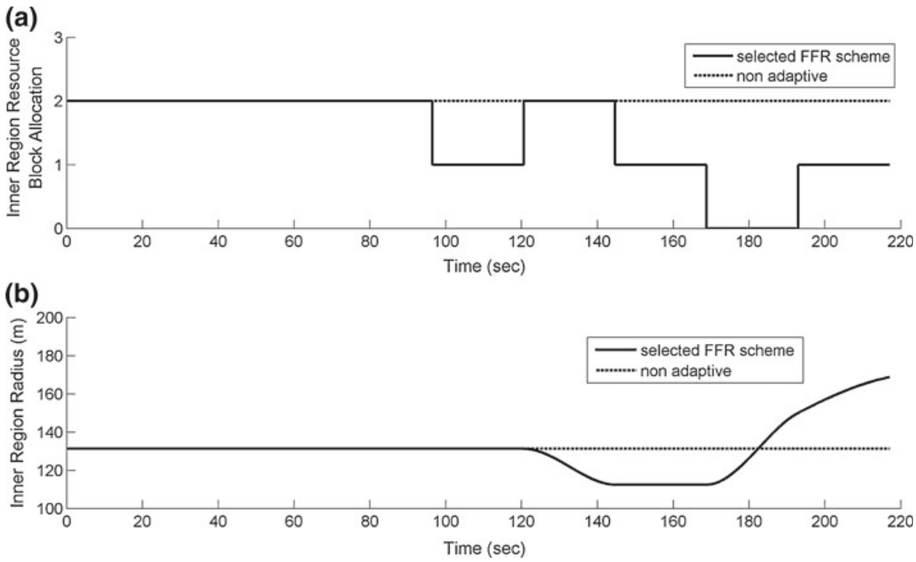


**Fig. 7** **a** Inner region RBs' allocation and **b** inner region radius versus time with and without the adaptation process

that lasts for 217 s the 24 users of the examined cell are moving randomly inside the cell with speed 3 km/h, according to the Pedestrian A channel model [26]. It is assured that all of them remain into the cell's area, ensuring that their total number will remain constant.

#### *6.3.1 Scenario 2: Selection and Update of Optimal FFR Scheme*

As the users move throughout the cell, the proposed mechanism adapts the range and the RBs' allocation of the inner region in order to ensure that all users in the cell will experience similar values of throughput. In Fig. 7, the "proposed mechanism" curves reflect this behaviour whereas the "non adaptive case" curves present the mechanism's performance without the adaptation process. More precisely, Fig. 7a depicts the inner region RBs' allocation and Fig. 7b presents the range of the inner region area against the time.

We remind that during the adaptation process, the mechanism updates the frequency allocation and inner region radius in order to take into account the users' mobility. The case without adaptation, on the contrary, assumes that the inner region frequency and radius are calculated once (for the initial user distribution) and remain constant during the scenario. This is reflected in Fig. 7a, where the non-adaptive case assigns the number of RBs in that way, so that as the time passes by, the RBs' allocation remains the same. On the other hand, the proposed mechanism updates the number of RBs allocated in the inner region so as to achieve the optimal US values. More specifically, we can observe that it updates the RBs' allocation for the first time 96.5 s after the experiment begins and keeps updating the RBs' allocation throughout the experiment in order to ensure that the US will keep the maximum value possible.

Similarly, Fig. 7b presents the mechanism's behavior as far as the inner region radius is concerned. For the first 120 s of the scenario the inner region radius remains constant. After

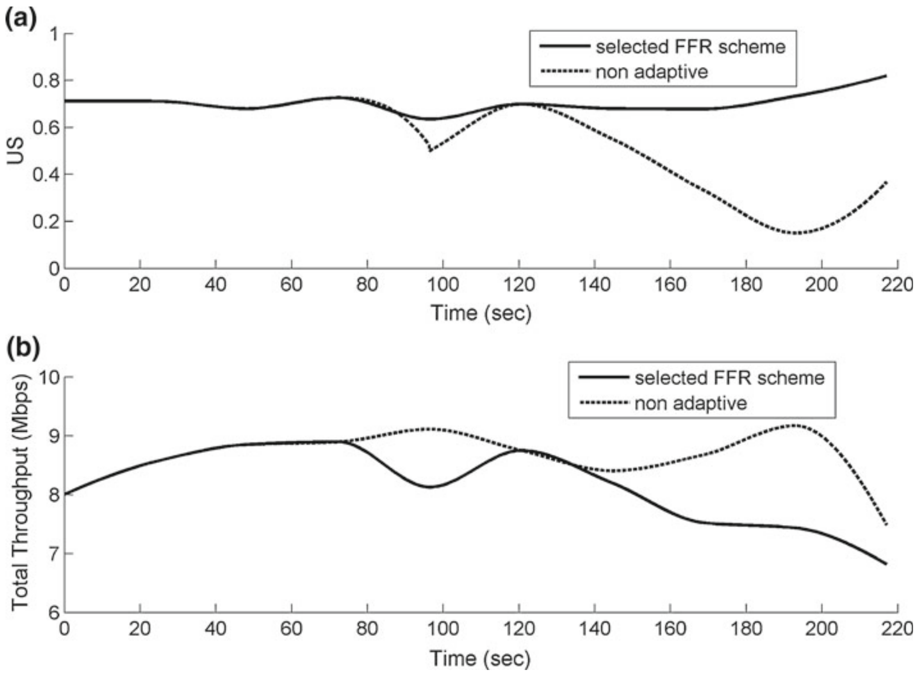


**Fig. 8** **a** US and **b** cell total throughput versus time with and without the adaptation process

this time interval, the mechanism adapts the inner region radius in order to reflect the users' movement and to achieve the maximum US value. On the other hand, when the adaptation process is not applied the radius of the inner region is calculated in the beginning of the experiment and does not change throughout the scenario.

Figure 8a confirms these results and illustrates the effectiveness of the adaptation process by presenting the US against time for the two cases (with and without the adaptation process). Indeed, during the experiment the values of US with adaptation are always higher (or equal) than the corresponding values when adaptation is not applied. For the first 96.5 s of the experiment the two curves coincide. After this time interval, the US of the non-adaptive case decreases rapidly while the US of the FFR scheme that is selected by the proposed mechanism remains at the same levels. In combination with Fig. 7, this happens because at simulation time 96.5 s, the mechanism updates the inner region RBs' allocation in order to reflect the users' mobility. This frequency re-allocation leads to higher values of US. Figure 8a also confirms that for the time interval between 120 s until the end of the experiment, the adaptation process contributes in keeping the value of US as high as possible. During this time interval the proposed mechanism updates both the inner region radius and the RBs' allocation (see Fig. 7) and compared to the non adaptive case results in higher US values.

For comparison purposes, Fig. 8b shows the corresponding curves of the cell total throughput. It is interesting to observe that even though the adaptation process leads to improved performance in terms of US, it results in lower (or equal) total throughput. This fact indicates that it allocates the bandwidth "equally" and in a fair way so that all users will experience similar throughput. The paragraph that follows includes, among others, a figure that shows the per-user throughput in order to further explain the advantages of having high US values.

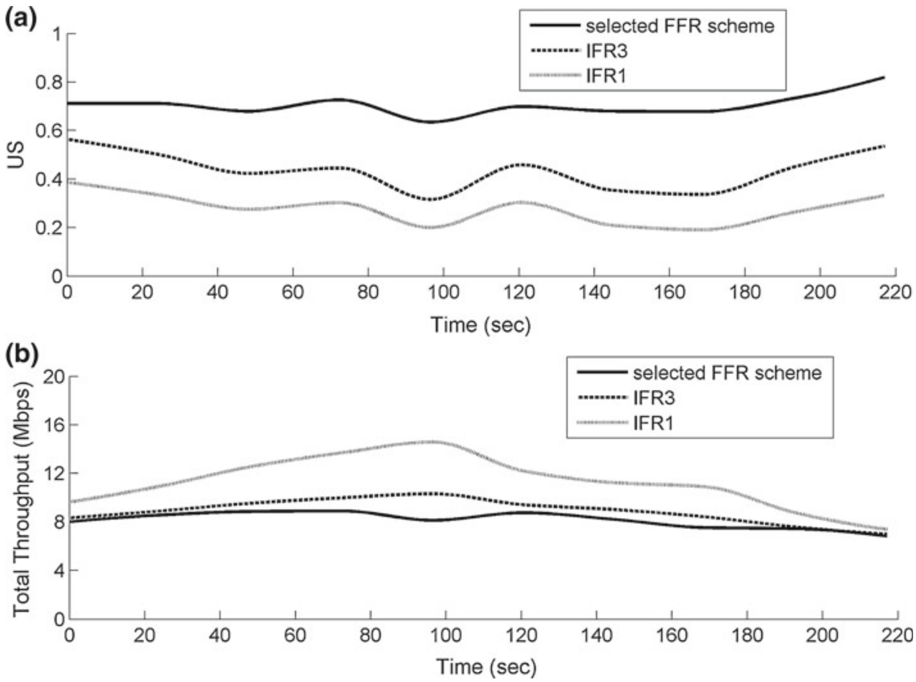


**Fig. 9** **a** US and **b** cell total throughput comparison of the three schemes (IFR1, IFR3 and selected FFR scheme)

*6.3.2 Scenario 2: Comparison of Selected FFR Scheme with IFR1 and IFR3*

In this section we present a direct comparison between IFR1, IFR3 and the selected FFR scheme for the mobility scenario. Figure 9a presents the US metric and Fig. 9b the cell total throughput against time for all approaches. According to Fig. 9a, the selected FFR scheme is the most efficient in terms of US. It achieves a maximum US value equal to 0.8189 (at the end of the experiment) whereas the IFR3 scheme achieves 0.5639 and IFR1 achieves 0.3867.

As far as the cell total throughput is concerned (Fig. 9b), we can observe that the selected (and updated) FFR scheme achieves a maximum throughput of 8.90 Mbps (at the 72nd s of the experiment). IFR1 achieves the highest total throughput value, which equals to 14.58 Mbps and the second highest total throughput is achieved by IFR3 (10.31 Mbps).

In order to reveal the impact of the US maximization and in order to further compare the three frequency reuse schemes, we examine the maximum, average, and minimum user throughput that each scheme achieves (Fig. 10a–c, respectively). As Fig. 10a, b depict, IFR1 achieves the highest values for the maximum and average user throughput throughout the simulation, while the selected FFR scheme achieves lower maximum and average values, which are close to the ones achieved by the IFR3. According to Fig. 10c, the selected FFR scheme achieves the highest minimum user throughput among the three frequency reuse schemes. It is very interesting to observe, that the curves that correspond to the maximum, average and minimum throughput of the FFR scheme that is selected by the proposed mechanism are very close. This means that the mechanism assigns similar values of throughput to the users irrespectively of the region that they are located (inner or outer).

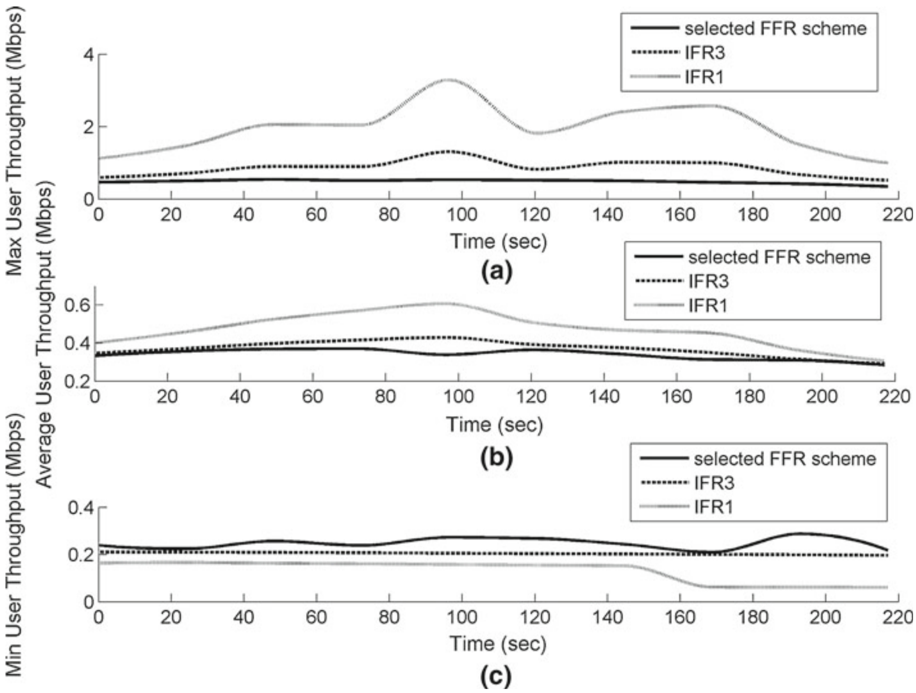


**Fig. 10** **a** Maximum, **b** average and **c** minimum user throughput versus time for the three schemes

To sum up, the proposed mechanism may lead to lower average cell total throughput values compared to the other two schemes; however, it allocates the available bandwidth between the two regions of the cell (inner and outer) in a "fairer" way so that all users in the cell experience similar throughput.

The above observations are clearly depicted in Fig. 11 that shows the throughput of the 24 users of the cell for the initial distribution (also see Fig. 3). This figure also corresponds to time slot 0 s in Fig. 10. According to Fig. 11, the selected FFR scheme ensures that all users will experience similar values of throughput regardless of their location in the cell. More precisely, it achieves the lowest throughput for the 2nd user (0.24 Mbps) and the highest for the 15th user (0.47 Mbps).

On the other hand, IFR1 allocates the available bandwidth in a quite "unfair" way. In this case, as Fig. 11 shows, six users (users 2, 4, 10, 11, 17 and 23) experience high throughput values, while the rest of them obtain lower values. The combination of Figs. 3 and 11 reveals that these users are located close to the base station. Therefore, IFR1 favours the users that are located close to the base station (1.12 Mbps throughput for user 17 that is closest to the base station) while the users are the cell edge experience lower throughput values (0.16 Mbps for user 9).

IFR3 allocates the available bandwidth in a similar way. Indeed, users 2, 4, 10, 11, 17 and 23, which are close to the base station, obtain the highest throughput values (0.59 Mbps for user 17), while user 8 that is at cell borders achieves the lowest (0.21 Mbps).

To summarize, the "fairest" throughput assignment is achieved by the proposed mechanism due to the RBs' allocation between the inner and outer cell region. The mechanism ensures that all the users will experience comparable values of throughput irrespective of their location in the cell.

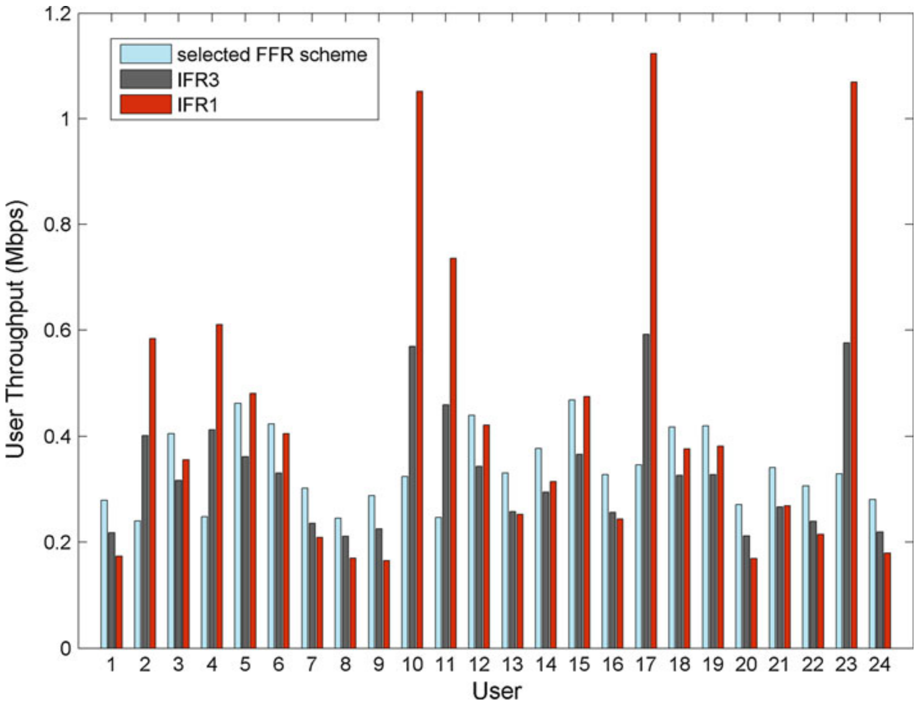


**Fig. 11** Per-user throughput of the three schemes for the initial distribution at 0 s

## 7 Conclusion

Interference avoidance in OFDMA systems through intelligent resource allocation is a technique to improve overall system capacity. The general approach to the interference avoidance problem, followed in this manuscript, is a dynamic mechanism that calculates the per-user SINR, capacity and throughput. After the above calculations, the mechanism selects the FFR scheme that maximizes the US metric. In order to take into account user's mobility in the topology, the proposed mechanism performs an adaptation process. During the adaptation process, the per-user throughput, the cell total throughput and US are re-calculated in periodic time intervals ensuring that at each time interval, the FFR scheme that maximizes the US metric is selected.

For the performance evaluation of the proposed mechanism, we distinguished two scenarios: one for a topology with static users and one for moving users. In the case of static users the cell total throughput and US were examined against network parameters such as inner region radius and bandwidth. Moreover, a comparison between IFR1, IFR3 and the FFR scheme that is selected by the proposed mechanism and was performed. According to the results the proposed mechanism achieves the maximum US value and therefore avoids to distinct between "high-throughput" and "low-throughput" users.

In the moving users' scenario, initially we compared the cases where the mechanism performs the adaptation process or not. The results indicated that the adaptation process leads to improved performance since it allows the update of inner region radius and frequency allocation and therefore can reflect the users' mobility. Moreover, we compared the performance of the FFR scheme that is selected by the proposed mechanism with the IFR1 and

IFR3 schemes. The comparison showed that the selected FFR scheme leads to lower cell total throughput values; however, it results in higher US vales. The overall observation is that the proposed mechanism allocates the available bandwidth between the two regions of the cell (inner and outer) in a more fair way, ensuring that all users in the cell will experience similar throughput.

## 8 Future Work

There are several steps that could follow this work. One potential step could be the optimization of the mechanism in order to minimize the scanning process and reduce its complexity. Indeed, assuming pedestrian users, it is expected that the new users' positions will be close to the initial ones. Therefore, it is expected to have small changes in the optimal frequency allocation and the optimal radius of the inner region. In brief, the optimized mechanism could reduce the scanning procedure after taking into account the "expected" frequency allocation and "expected" inner region radius.

Femtocells are data access points installed by the subscribers so as to provide better indoor voice and data coverage and to increase system capacity. One of the major technical challenges that femtocell networks are facing is their interference behaviour when they are placed within macrocells. Motivated by the fact that femtocells are expected to be one of the emerging technologies for the next generation communication systems, a future step would be the extension of the proposed mechanism in order to incorporate femtocells. The extended mechanism could provide an efficient method to utilize the unused frequency bands of the macrocell for femtocells in order to avoid the co-channel interference and therefore increase the performance of the system.

Finally, the investigation of the impact of scale and varying mixes of traffic on the overall performance of the proposed mechanism could constitute a future step. Indeed, there are many important aspects of cellular traffic that could be examined. These aspects include traffic capacity and cell size, quality of service targets, spectral efficiency and cell sectoring or traffic capacity versus coverage.

## References


1. Mobile WiMAX-Part, II. (2006). *A comparative analysis. Tech. Rep., WiMAX Forum*, May 2006.
2. Necker, M. C. (2007). Local interference coordination in cellular OFDMA networks. In proceedings of *IEEE 66th vehicular technology conference* (VTC 2007-Fall) (pp. 1–5). Stuttgart, Germany.
3. FFR Scheme Selection Mechanism. Available at http://ru6.cti.gr/ru6/FFR_selection_mechanism.zip.
4. 3GPP. (2005). *Radio access network work group1 contributions*. http://www.3gpp.org.
5. Begain, K., Rozsa, G. I., Pfening, A., & Telek, M. (2002). Performance analysis of GSM networks with intelligent underlay-overlay. In *Proceedings of the 7th international symposium on computers and communications (ISCC 2002)* (pp. 135–141), Taormina, Italy.
6. Mobile WiMAX Part I. (2006). *A technical overview and performance evaluation, WiMAX Forum*. *Tech. Rep*. February 2006.
7. 3GPP TSG RAN WG1#42 R1–050841. (2005). *Further analysis of soft frequency reuse scheme*. *Huawei, Tech. Rep.,*
8. 3GPP TSG RAN WG1#42 R1–050764. (2005). *Inter-cell interference handling for E-UTRA, Ericsson*. *Tech. Rep.* September 2005.
9. Chang, R. Y., Tao, Z., Zhang, J., & Kuo, C.-C. J. (2009). A graph approach to dynamic fractional frequency reuse (FFR) in multi-cell OFDMA networks, In *proceedings of IEEE international conference on communications (ICC 2009)* (pp. 1–6). Dresden, Germany.

10. Assad, M. (2008). Optimal fractional frequency reuse (FFR) in multicellular OFDMA system. In *proceedings of IEEE 68th vehiculear technology conference (VTC 2008–Fall)* (pp. 1–5). Colgay, Canada.
11. Hassan, N. U. L., & Assad, M. (2009). Optimal fractional frequency reuse (FFR) and resource allocation in multiuser OFDMA system. In *proceedings of international conference on information and communication technologies, (ICICT 2009)* (pp. 88–92). Karachi, Pakistan.
12. Fang, L., & Zhang, X. (2008). Optimal fractional frequency reuse in OFDMA based wireless networks. In *Proceedings of 4th international conference on wireless communications, networking and mobile. computing, (WiCOM'08)* (pp. 1–4) Dalian, china.
13. Xiang, Y., & Luo, J. (2007). Inter-cell interference mitigation through flexible resource reuse in OFDMA based communication networks. In *Proceedings of European Wireless' 2007* (pp. 1–7). Paris, France.
14. 3GPP TSG RAN WG1 Meeting #41 R1–050507. (2005). *Soft frequency reuse scheme for UTRAN LTE*. Huawei, Athens, Greece, May 2005.
15. Sternad, M., Ottosson, T., Ahlen, A., & Svensson, A. (2003). Attaining both coverage and high spectral efficiency with adaptive OFDM downlinks. In *Proceedings of IEEE 58th Vehicular Technology Conference (VTC 2003-Fall)* (Vol. 4, pp. 2486–2490).
16. Fodor, G., Koutsimanis, C., Rácz, A., Reider, N., Simonsson, A., & Müller, W. (2009). Intercell interference coordination in OFDMA networks and in the 3GPP long term evolution system. *Journal of Communications*, *4*(7), 445–453.
17. Li, G., & Liu, H. (2006). Downlink radio resource allocation for multi-cell OFDMA system. *IEEE Transactions on Wireless Communications, 5*(12), 3451–3459.
18. Godlewski, Ph., Maqbool, M., Coupechoux, M., & Kelif, J. M. (2008). Analytical evaluation of various frequency reuse schemes in cellular OFDMA networks. In *Proceedings of 3rd international conference on performance evaluation methodologies and tools (Valuetools 2008)* (pp. 1–10). Athens, Greece.
19. 3GPP TSG-RAN, TR 25.814. (2006–2005). *Physical layer aspects for evolved UTRA (Release 7)*, v1.3.1.
20. Lei, H., Zhang, L., Zhang, X., & Yang, D. (2007). A novel multi-cell OFDMA system structure using fractional frequency reuse. In *Proceedings of IEEE 18th international symposium on personal, indoor and mobile radio communications (PIMRC'07)* (pp. 1–5). Athens, Greece.
21. Bilios, D., Bouras, C., Kokkinos, V., Papazois, A., & Tseliou, G. (2012). Optimization of fractional frequency reuse in long term evolution networks. In *Proceeding of IEEE wireless communications and networking conference (WCNC 2012)* (pp. 1853–1857). Paris, France.
22. 3GPP TR 36.814 V9.0.0. (2010). *Technical report 3rd generation partnership project; Technical specification group radio access network; Evolved universal terrestrial radio access (E-UTRA); Further advancements for E-UTRA physical layer aspects (Release 9)*, March 2010.
23. 3GPP. (2009). LTE Resource Guide. Anritsu Company.
24. Shabbir, N., Sadiq, M. T., Kashif, H., & Ullah, R. (2011). Comparison of radio propagation models for long term evolution (Lte) network. *International Journal of Next-Generation Networks (IJNGN), 3*(3), 27–41.
25. Saunders, S. (2000). *Antennas and propagation for wireless communication systems*. Wiley.
26. ITU-R M.1225 International Telecommunication Union. (1997). *Guidelines for evaluation of radio transmission technologies for IMT-2000*.


## Author Biographies

**Dimitrios Bilios** was born in Athens, Greece in 1989. He entered the Computer Engineering and Informatics Department in 2006 and joined the Research Unit 6 of Computer Technology Institute and Press "Diophantus" in 2011. He has obtained State Certificate of Foreign Language Proficiency (Level: independent user-B2) in English and Zertifikat Deutch in German. Currently, he is an undergraduate student and he is interested in open source development, mobile telecommunication networks and frequency reuse techniques.

**Christos Bouras** is Professor in the University of Patras, Department of Computer Engineering and Informatics. Also he is a scientific advisor of Research Unit 6 in Computer Technology Institute and Press—Diophantus, Patras, Greece. His research interests include Analysis of Performance of Networking and Computer Systems, Computer Networks and Protocols, Telematics and New Services, QoS and Pricing for Networks and Services, e-learning, Networked Virtual Environments and WWW Issues. He has extended professional experience in Design and Analysis of Networks, Protocols, Telematics and New Services. He has published more than 400 papers in various well-known refereed books, conferences and journals. He is a co-author of 9 books in Greek and editor of 1 in English. He has been a PC member and referee in various international journals and conferences. He has participated in R&D projects. He is member of experts in the Greek Research and Technology Network (GRNET), member of Scientific Committee og GRNET, member of Strategic Committee of Digital Greece 2020, also he is member of BoD of GFOSS, member of Central Committee of TEE and BoD of e-TEE (Vice President).

**Vasileios Kokkinos** obtained his diploma from the Physics Department of the University of Patras on October 2003. Next, he was accepted in the postgraduate program "Electronics and Information Processing" in the same department and on March 2006 he obtained his Master Degree. In 2010 he received his Ph.D. on Power Control in Mobile Telecommunication Networks from the Computer Engineering and Informatics Department. He works in the Research Unit 6 of Computer Technology Institute and Press "Diophantus" since September 2006. His research interests include data networks, third and fourth generation mobile telecommunications networks, multicast routing and group management and radio resource management. He has obtained the Cambridge Proficiency in English and the Zertifikat diplom in German. He has published more than 40 research papers in various well-known refereed conferences and scientific journals.

**Andreas Papazois** obtained his diploma, M.Sc. and Ph.D. from Computer Engineering and Informatics Dept., University of Patras, Greece. He is currently an R&D engineer at Research Unit 6: Networks Telematics and New Services, Computer Technology Institute and Press—Diophantus. He has also worked as Telecommunication Systems Engineer in Intracom Telecom S.A. His research interests include Web Services, Mobile Telecommunication Networks, Error Control techniques, Quality of Service and Multicast Transmission. He has published several research papers in various well-known refereed conferences, books and scientific journals. He has also been a reviewer for various international journals and conferences.

**Georgia Tseliou** was born in Lamia, Greece in 1989. She entered the Computer Engineering and Informatics Department in 2007 and joined the RU6 in 2010. Her research interests include Mobile Telecommunication networks, Broadcast and Multicast Transmission, Radio Resource Management and Frequency Reuse techniques. She has obtained Cambridge and Michigan Proficiency in English, Delf B2 in French and Dele B2 in Spanish. She has participated in several projects run by Computer Technology Institute and Press "Diophantus", Patras, Greece.